

Pseudoentanglement from tensor networks

Zihan Cheng, Xiaozhou Feng, and Matteo Ippoliti

Department of Physics, The University of Texas at Austin, Austin, TX 78712, USA

Pseudoentangled states are defined by their ability to hide their entanglement structure: they are indistinguishable from random states to any observer with polynomial resources, yet can have much less entanglement than random states. Existing constructions of pseudoentanglement based on phase- and/or subset-states are limited in the entanglement structures they can hide: e.g., the states may have low entanglement on a single cut, on all cuts at once, or on local cuts in one dimension. Here we introduce new constructions of pseudoentangled states based on (pseudo)random tensor networks that affords much more flexibility in the achievable entanglement structures. We illustrate our construction with the simplest example of a matrix product state, realizable as a staircase circuit of pseudorandom unitary gates, which exhibits pseudo-area-law scaling of entanglement in one dimension. We then generalize our construction to arbitrary tensor network structures that admit an isometric realization. A notable application of this result is the construction of pseudoentangled ‘holographic’ states whose entanglement entropy obeys a Ryu-Takayanagi ‘minimum-cut’ formula, answering a question posed in [Aaronson *et al.*, arXiv:2211.00747].

Introduction. Entanglement is a fundamental resource in quantum information science and an important principle in theoretical physics, from condensed matter to gravity [1–8]. At the same time, the entanglement structure of large many-body states is very challenging to observe. Specifically, there exist N -qubit states with very low entanglement that are *computationally indistinguishable* (i.e., indistinguishable to any observer whose resources scale polynomially in N) from states with much higher entanglement, such as Haar-random states. This property is known as pseudoentanglement [9–11].

Motivated originally by ideas in quantum cryptography [12], the concept of pseudoentanglement enables connections to many-body physics in contexts including thermal equilibrium in many-body dynamics [13], learning of Hamiltonian ground states [11], and holography [9], where it may have implications for the complexity of the AdS/CFT “dictionary” [14]. In general, it is a powerful tool to demonstrate the existence of entanglement structures that are computationally inaccessible, and thus contributes to sharpen the limits of what is learnable in realistic quantum experiments.

Existing constructions of pseudoentangled state ensembles are based on subset-phase-states, $|\psi_{\mathcal{S},f}\rangle \propto \sum_{x \in \mathcal{S}} (-1)^{f(x)} |x\rangle$, where under suitable constraints on the Boolean function $f : \{0, 1\}^N \rightarrow \{0, 1\}$ and/or the subset $\mathcal{S} \subseteq \{0, 1\}^N$ one can prove computational pseudorandomness and enforce an upper bound on entanglement either on specific cuts or on all cuts at once [9, 10]. These constructions are very powerful and in some cases achieve the theoretical maximum amount of hideable entanglement. However, they natively represent unstructured states where all N qubits are on the same footing, without e.g. a notion of locality. This makes them well suited to emulate maximally random states such as those that describe infinite-temperature equilibrium [13], but limits their ability to mimic more structured systems. While it is possible to tailor phase-states to reflect some locality structure [11], it remains not clear in general how to mimic physical systems of interest, such as holographic

ones.

Motivated by these considerations, in this work we introduce new families of pseudoentangled states with a highly flexible entanglement structure. We leverage tensor networks [15–19], which allow us to hard-code locality and the associated entanglement (pseudo-)area-law into our states. Recently proposed efficient constructions of pseudorandom unitaries [20] then allow for the efficient preparation of pseudoentangled states whose true (computationally hidden) entanglement structure is that of an arbitrary tensor network that admits an *isometric* realization [17, 19, 21, 22]. These include many examples of interest, from matrix product states (MPS) to projected entangled pair states (PEPS) in any dimension [15, 23, 24] and even holographic tensor network states [18, 25–27].

Pseudoentanglement.—An ensemble of pure quantum states \mathcal{E} is pseudoentangled if [9] (i) it is efficiently preparable, (ii) it is computationally indistinguishable from the Haar-random state ensemble, and (iii) it has abnormally low entanglement entropy on some cuts. Formally, computational indistinguishability is stated as follows: for all $m \leq O(\text{poly}(N))$ and any efficient algorithm [28] \mathcal{A} , one has

$$\left| \mathcal{A}(\rho_{\mathcal{E}}^{(m)}) - \mathcal{A}(\rho_{\text{Haar}}^{(m)}) \right| \leq o(1/\text{poly}(N)), \quad (1)$$

in terms of the ‘moment operators’ $\rho_{\mathcal{E}}^{(m)} = \mathbb{E}_{\psi \sim \mathcal{E}} [|\psi\rangle\langle\psi|^{\otimes m}]$. This means that an observer with access to polynomially many copies m of a given state would have no way of deciding which ensemble it came from in polynomial time. The constraint on entanglement is simply that, for some extensive subsystem A and with high probability over the state $\psi \sim \mathcal{E}$, the entanglement entropy $S(A)$ is bounded above by a function $f(N) \leq o(N)$. By comparison, the scaling of entanglement entropy in Haar-random states (known as the Page curve [29]) is $S(A) = \Theta(N)$ for any extensive subsystem. The discrepancy between true and apparent entanglement is called the pseudoentanglement gap.

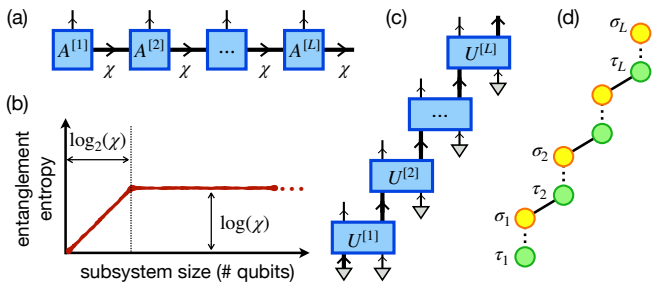


FIG. 1. Construction of pseudoentangled MPS. (a) Diagrammatic representation of a MPS. Thin and thick lines represent qubits and χ -state qudits, respectively; the $A^{[j]}$ tensors are isometries in the direction specified by the arrows. (b) Entanglement entropy of a typical random MPS for contiguous cuts of the qubit chain. (c) Realization of the MPS as a staircase unitary circuit. Triangles represent auxiliary qubits in the $|0\rangle$ state. (d) Partition function that controls the m -th moment of the random MPS ensemble. Each gate turns into two S_m -valued spins, with a 1D interaction graph.

The theoretically maximal pseudoentanglement gap is $f(N) = \omega(\log N)$ vs $\Theta(N)$, and can be saturated by random subset-phase states [9–11].

Pseudoentangled matrix product states.—We first exhibit our construction on the simplest tensor network: the one-dimensional matrix product state (MPS). A MPS, sketched in Fig. 1(a), is a many-body state whose amplitudes are expressed as $\langle i_1, \dots, i_N | \psi \rangle = \text{Tr}(A_{i_1}^{[1]} \cdots A_{i_N}^{[N]})$, with each $A_{i_j}^{[j]}$ a $\chi \times \chi$ matrix; χ is a numerical cut-off known as the *bond dimension*, which upper-bounds the Schmidt rank of the state about any bond on the 1D line and thus imposes an area-law, Fig. 1(b). A standard route to prepare MPSs in the lab is to use ‘staircase’ circuits [30], where one associates $A_{i,\alpha,\beta}^{[j]} = \langle i, \beta | U^{[j]} | 0, \alpha \rangle$, with $U^{[j]}$ a unitary gate acting on a qubit and a χ -state qudit. This is sketched in Fig. 1(c). In this work we take $\chi = 2^\nu$, so each $U^{[j]}$ is a $(\nu + 1)$ -qubit gate. The staircase circuit comprises L gates; for the last gate, all $\nu + 1$ output qubits become part of the physical system, which in all is made of $N = L + \nu$ qubits. We take our unitary gates $\{U^{[j]}\}_{j=1}^L$ to be drawn from the recently introduced ‘PFC ensemble’ [20] of pseudorandom unitaries (PRUs). These are efficiently implementable transformations that are computationally indistinguishable from Haar-random unitaries (see [31], [20] for more details). We denote the resulting ensemble of N -qubit pure states by $\mathcal{E}_{\text{pMPS}}$.

Our first main result is that, given a sufficiently large bond dimension, this ensemble is pseudoentangled:

Theorem 1. *If $\omega(\text{poly}(N)) \leq \chi \leq 2^{o(N)}$, the pseudo-random MPS ensemble $\mathcal{E}_{\text{pMPS}}$ is pseudoentangled.*

Efficient preparability of this ensemble is clear—it is the sequential application of $O(N)$ efficient PRUs. Limited entanglement follows from the MPS structure: cutting any bond on the line yields entanglement $\leq \log(\chi)$,

which is by assumption $o(N)$. It remains to prove computational indistinguishability from the Haar-random state distribution.

We split this task in three parts. First, by definition of the PFC ensemble [20], the pseudorandom ensemble $\mathcal{E}_{\text{pMPS}}$ is computationally indistinguishable from its counterpart $\mathcal{E}_{\text{pMPS}'}$ where the pseudorandom PFC gates are replaced by genuinely random permutations, phase, and Clifford gates. Next, we prove that $\mathcal{E}_{\text{pMPS}'}$ is indistinguishable from its counterpart made of genuine Haar-random gates, which we term $\mathcal{E}_{\text{rMPS}}$:

Lemma 1. *We have $\|\rho_{\mathcal{E}_{\text{pMPS}'}}^{(m)} - \rho_{\mathcal{E}_{\text{rMPS}}}^{(m)}\|_{\text{tr}} \leq O(Nm/\sqrt{\chi})$.*

The proof of this fact follows easily from the properties of the PFC ensemble, and is reported in [30]. We finally show that the random MPS ensemble $\mathcal{E}_{\text{rMPS}}$ is indistinguishable from the Haar-random ensemble:

Lemma 2. *We have $\|\rho_{\mathcal{E}_{\text{rMPS}}}^{(m)} - \rho_{\text{Haar}}^{(m)}\|_{\text{tr}} \leq O(Nm^2/\chi)$.*

Proof. Let us first recall two facts about the Haar measure:

- (i) the m -th moment of the Haar measure over states is given by $\rho_{\text{Haar}}^{(m)} = f_{q,m} \sum_{\sigma \in S_m} \hat{\sigma}$, with $\hat{\sigma}$ the replica permutation operator associated to permutation $\sigma \in S_m$, q the Hilbert space dimension, and $f_{q,m} = (q-1)!/(q+m-1)!$;
- (ii) the m -th twirling channel for the Haar measure is given by $\Phi_{\text{Haar}}^{(m)}(O) = \mathbb{E}_{U \sim \text{Haar}}[U^{\otimes m} O (U^\dagger)^{\otimes m}] = \sum_{\sigma, \tau \in S_m} \text{Wg}_q(\sigma\tau^{-1}) \text{Tr}(O\hat{\tau}) \hat{\sigma}$, where $\text{Wg}_q(\sigma\tau^{-1})$ is the Weingarten function, see [30].

Carrying out the Haar averages with these tools, we see that the m -copy distinguishability between $\mathcal{E}_{\text{rMPS}}$ and $\mathcal{E}_{\text{Haar}}$ reads

$$\Delta_m \equiv \left\| f_{D,m} \sum_{\sigma} \hat{\sigma}^{\otimes L} - \sum_{\{\sigma_i, \tau_i\}} e^{-E[\{\sigma_i, \tau_i\}]} \bigotimes_{i=1}^L \hat{\sigma}_i \right\|_{\text{tr}} \quad (2)$$

where $D = 2^N$ is the physical Hilbert space dimension, each $\hat{\sigma}$ denotes a replica permutation for a single qubit ($i < L$) or 2χ -state qudit ($i = L$), and $e^{-E[\{\sigma_i, \tau_i\}]}$ is a ‘Boltzmann weight’ (not necessarily positive) of a configuration of S_m -valued spins on a line, sketched in Fig. 1(d). This way of writing the operator is reminiscent of a partition function [32] and will be helpful in our analysis.

Using the triangle inequality, we bound the distinguishability measure as $\Delta_m \leq \Delta_m^{\text{u.}} + \Delta_m^{\text{n.u.}}$, in terms of uniform and non-uniform spin configurations:

$$\Delta_m^{\text{u.}} = \left\| \sum_{\sigma \in S_m} [f_{D,m} - e^{-E[\{\sigma, \sigma\}]}] \hat{\sigma}^{\otimes L} \right\|_{\text{tr}}, \quad (3)$$

$$\Delta_m^{\text{n.u.}} = \left\| \sum_{\{\sigma_i, \tau_i\} \text{ n.u.}} e^{-E[\{\sigma_i, \tau_i\}]} \bigotimes_{i=1}^L \hat{\sigma}_i \right\|_{\text{tr}}, \quad (4)$$

with ‘n.u.’ denoting a restriction to non-uniform configurations (where not all σ_i, τ_i coincide).

We first show that Δ_m^u is small. The Boltzmann weight of the uniform spin configuration is $e^{-E[\{\sigma, \sigma\}]} = \chi^{L-1} \text{Wg}_{2\chi}(e)^L$ (independent of σ), with e the identity permutation. We show in [30] that $\text{Wg}_{2\chi}(e) = (2\chi)^{-m} [1 + O(m^2/\chi)]$; therefore $e^{-E[\{\sigma, \sigma\}]} = D^{-m} [1 + O(m^2/\chi)]$. At the same time, by the ‘birthday asymptotics’ we have $f_{D,m} = D^{-m} [1 + O(m^2/\chi)]$, so overall

$$\Delta_m^u \leq \|\rho_{\text{Haar}}^{(m)}\|_{\text{tr}} \left| 1 - \frac{e^{-E[\{e, e\}]} }{f_{D,m}} \right| \leq O\left(\frac{m^2}{\chi}\right). \quad (5)$$

Next, we show that $\Delta_m^{\text{n.u.}}$, Eq. (4), is also small. We write $\bigotimes_{i=1}^L \hat{\sigma}_i = \hat{\sigma}_1^{\otimes L} \bigotimes_{i=1}^L \hat{\sigma}'_i$, where $\hat{\sigma}'_1 = e$ (identity permutation). Then, using the inequality $\|AB\|_{\text{tr}} \leq \|A\|_{\text{tr}} \|B\|_{\text{op}}$ to factor out the sum over σ_1 , we obtain

$$\Delta_m^{\text{n.u.}} \leq \|\rho_{\text{Haar}}^{(m)}\|_{\text{tr}} \left\| \sum_{\{\sigma'_i, \tau_i\} \text{ n.u.}} \frac{e^{-E[\{\sigma'_i, \tau_i\}]} }{f_{D,m}} \bigotimes_{i=1}^L \hat{\sigma}'_i \right\|_{\text{op}}. \quad (6)$$

Using the triangle inequality and the fact that $\|\hat{\sigma}\|_{\text{op}} = 1$ (unitarity of the replica permutations), we have

$$\Delta_m^{\text{n.u.}} \leq 2 \sum_{\{\sigma'_i, \tau_i\} \text{ n.u.}} e^{-(E^+[\{\sigma'_i, \tau_i\}] - E^+[\{e, e\}])}. \quad (7)$$

Here we defined positive Boltzmann weights $e^{-E^+[\{\sigma'_i, \tau_i\}]} \equiv |e^{-E[\{\sigma'_i, \tau_i\}]}|$, and used the fact that $f_{D,m} \simeq e^{-E^+[\{e, e\}]} \geq e^{-E^+[\{e, e\}]} / 2$ (as seen in the discussion of Δ_m^u) to subtract the ground state energy $E^+[\{e, e\}]$.

Having pinned the $\hat{\sigma}'_1$ site spin, we are free to move to bond spin variables: $\beta_\ell = \alpha_i \alpha_j^{-1}$ for each bond $\ell = (i, j)$. Each bond sum has a unit contribution from the bond ground state, $\beta_\ell = e$, while excited states $\beta_\ell \neq e$ are suppressed by powers of $1/\chi$. We show in [30] that each such sum yields $1 + O(m^2/\chi)$. Overall, $\Delta_m^{\text{n.u.}} \leq 2[1 + O(m^2/\chi)]^{2L} - 1 \leq O(Nm^2/\chi)$. \square

Eq. (7) has an intuitive physical interpretation: the right hand side represents thermal fluctuations of a genuine lattice magnet (with real energy levels); pinning the value of $\sigma_1 = e$ removes the giant $m!$ degeneracy of the ground state, and restricting the sum to non-uniform configurations $\{\sigma'_i, \tau_i\}$ further removes the (now unique) ground state $\sigma'_i = \tau_i = e$, so that the remaining sum quantifies thermal fluctuations. Normally in 1D systems these would be large due to the lack of long range order at any finite temperature. However, the effective temperature of this magnet, controlled by the bond dimension χ as $1/\log(\chi)$, is being taken to zero as $o(1/\log(N))$ with increasing system size [since $\chi = \omega(\text{poly}(N))$]. In this regime long range order is possible even in 1D.

This result establishes that an isometric MPS made of random unitaries is a pseudorandom state if the bond dimension χ is superpolynomial in N . Further, it is clear that the entanglement entropy is bounded above

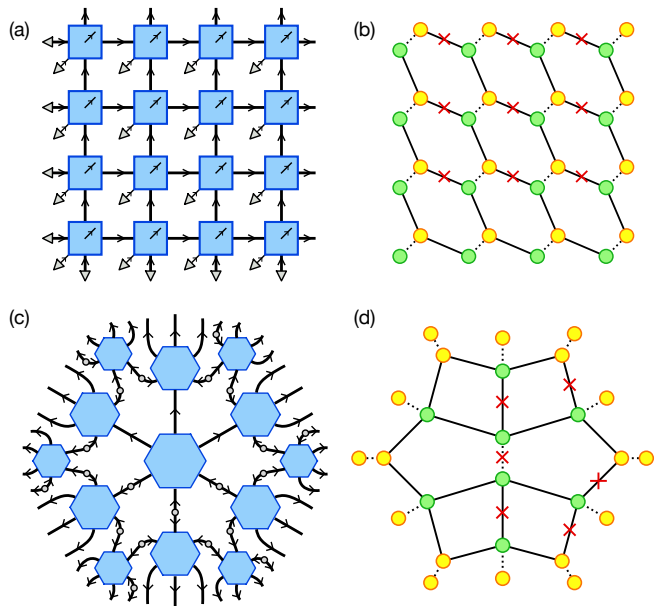


FIG. 2. Construction of pseudoentangled states based on arbitrary isometric tensor networks. (a-c) Isometric realization of a PEPS on a 2D square lattice and a holographic tensor network on a $\{6,4\}$ tiling of the hyperbolic plane. Arrows denote the direction of unitarity. Gray triangles in (a) are $|0\rangle$ states, gray circles in (c) are Bell pair states. Thin lines (in (a) only) are qubits, thick lines are χ -state qudits. (b-d) Partition functions obtained from averaging over Haar-random unitaries. Green and yellow sites represent ‘bulk’ spins (τ) and ‘boundary’ spins (σ), respectively. Solid bonds give overlaps between permutations, dashed bonds give Weingarten functions. Bonds marked by a \times can be dropped to obtain a spanning tree of the interaction graph, used in our proof of computational pseudorandomness.

by $|\partial A| \log_2(\chi)$ for any subsystem A , where ∂A is the boundary of A . For typical realizations, the entanglement entropy of a segment A of length ℓ scales linearly in ℓ up to $\ell \simeq \nu$, at which point it saturates. This saturation value is constant in ℓ but grows with total system size as $\omega(\log N)$, a behavior we may call ‘pseudo-area-law’, sketched in Fig. 1(b).

Pseudoentanglement in general isometric tensor networks. This construction is straightforwardly generalizable to other geometries beyond one dimension, e.g. to PEPS in 2D [15, 23], which can also be realized as isometric tensor networks [17] subject to some constraints on their bond dimensions, see Fig. 2(a-b). We generalize the proof for MPS given above to arbitrary isometric tensor networks in [30]; here we summarize the main idea.

The only element of the MPS proof that needs a non-trivial adjustment is the treatment of the partition function following Eq. (7), where the change of variables from site spins to bond spins exploited the loop-free 1D geometry of the MPS. However, since the Boltzmann weights $e^{-(E^+[\{\sigma'_i, \tau_i\}] - E^+[\{e, e\}])}$ can be written as products of bond terms that are all individually ≤ 1 (see [30] for more

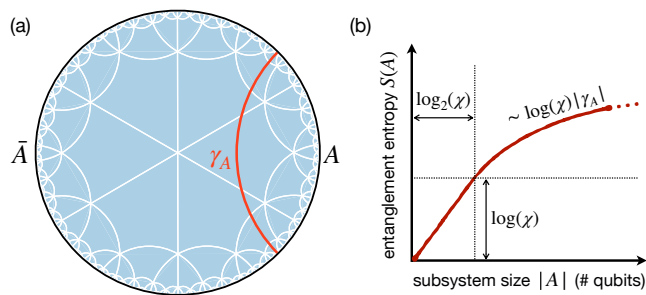


FIG. 3. (a) Schematic of minimum cut for the entanglement of a boundary interval A in a holographic tensor network. (b) Scaling of the entanglement entropy in holographic pseudoentangled states (here each χ -state qudit in the output state is split into $\nu = \log_2(\chi)$ qubits). A Page-like scaling $\sim |A| \log(2)$ extends up to $|A| \sim \log(\chi) = \omega(\log N)$, then the minimum cut $|\gamma_A|$ starts deviating from the volume $|A|$; in hyperbolic tilings one has $|\gamma_A| \sim \log |A|$ on large length scales.

details), the partition function is non-decreasing under removal of any given bond (i.e., replacing a bond term by 1). Thus we can upper-bound the partition function by dropping edges in the graph until we obtain a spanning tree, as sketched in Fig. 2(c-d); at this point we can change variables to bond spins (since the tree is free of loops) and conclude the proof as before.

Therefore our construction can realize pseudo-area-law entangled states on d -dimensional Euclidean lattices, where the entropy of contiguous subsystems obeys $S(A) \simeq \nu |\partial A|$, with $\nu = \log_2(\chi) = \omega(\log(N))$. Such states correctly track the Page curve as long as A is a ball of radius $O(\nu^{1/d})$ in the lattice, then switch to the area-law scaling.

Holographic tensor networks. An important application of our construction is to tensor network models of holography, where a quantum system is viewed as the “boundary” of a higher-dimensional “bulk” space, and its entanglement structure reflects the geometry of the bulk. These models [4, 18, 25, 26, 33, 34] have attracted considerable interest as toy models of the AdS/CFT correspondence and its links to quantum error correction. They generally feature tensors arranged on a tiling of 2D hyperbolic space, which may or may not have physical legs in the bulk, terminating with “dangling” legs on the boundary which represents the physical system of interest. Holographic tensor networks are very well suited to our construction, since they encode the bulk isometrically into the boundary; i.e., the tensor network may be viewed as a circuit propagating information unitarily outward from the center of the hyperbolic space toward its boundary. (We do not consider recently introduced *non-isometric codes* here, though that would be an interesting direction for future work [35, 36].)

Here we focus for concreteness on the $\{6, 4\}$ tiling of the hyperbolic plane with 6-leg tensors (3-qudit unitary gates), without bulk degrees of freedom. This is sketched in Fig. 2(b). Placing a PRU of dimension χ^3 on each

hexagon defines a state ensemble $\mathcal{E}_{\text{holo}}$. Our general proof extends to this ensemble and is sufficient to show pseudoentanglement: $\mathcal{E}_{\text{holo}}$ is computationally indistinguishable from Haar-random, while the entanglement entropy is bounded away from volume-law. The latter property follows, as in previous examples, from the limit on the Schmidt rank of the state imposed by the tensor network structure. Namely, we have $S(A) \leq \min_{\gamma_A} |\gamma_A| \log(\chi)$, where γ_A is a curve that separates A from \bar{A} in the network, and $|\gamma_A|$ is the number of bonds it cuts; see Fig. 3. Generally on hyperbolic tilings one has $\min_{\gamma_A} |\gamma_A| \sim \log |A|$, and thus sub-volume-law scaling, as claimed.

A key property of holographic states (and random circuits or tensor networks more generally [37–40]) is that their entropy approximately saturates the minimum-cut upper bound. Precisely, the Ryu-Takayanagi formula [41, 42] states that

$$S(A) = \frac{\min_{\gamma_A} |\gamma_A|}{4G} \quad (8)$$

where G is Newton’s constant in the bulk gravitational theory. We can prove that our ensemble $\mathcal{E}_{\text{holo}}$ is indeed holographic in this sense. In [30] we prove a lower bound on the average entropy which, together with the aforementioned upper bound from the Schmidt rank, yields the following:

Theorem 2. *For any subsystem A , the holographic pseudorandom tensor network ensemble $\mathcal{E}_{\text{holo}}$ obeys*

$$\mathbb{E}_{\psi \sim \mathcal{E}_{\text{holo}}} [S(A)] = |\gamma_A| \log(\chi) [1 + o(1)] + O(N/\chi). \quad (9)$$

Up to terms that vanish in the thermodynamic limit, this is a RT formula with “Newton’s constant” $G = 4/\log(\chi) = o(1/\log(N))$.

Discussion. We have constructed new models of pseudoentangled quantum state ensembles by combining pseudorandom unitaries and isometric tensor networks. Compared to prior constructions of pseudoentanglement, this approach provides more flexibility in the choice of entanglement structures that may be computationally hidden. These include pseudo-area-law scaling in any dimension as well as holographic entanglement which obeys a Ryu-Takayanagi formula, Eq. (9). The implications of our construction for holography remain to be explored, as well as possible extensions of our construction to more general and non-isometric holographic codes [35, 36].

Given the prominent role of tensor networks in many-body physics (from exact representations of local Hamiltonian ground states to variational ansätze for time evolution to models of holography) this approach facilitates the integration of computational pseudorandomness in diverse physical settings. This paves the way for applications to the hardness of learning various properties of structured many-body states, such as Hamiltonian eigenstates or states prepared by specific types of non-thermalizing quantum dynamics. We leave these interesting directions to future work.

Note added. While working on this manuscript we became aware of a forthcoming work by Akers, Bouland, Chen, Kohler, Metger and Vazirani [43] that introduces a different construction of holographic pseudoentangled states. Additionally, during or after completion of this manuscript, several related works appeared on arXiv: Ref. [44] by Engelhardt et al introduced a different construction of pseudoentangled holographic states; Ref. [45] by Schuster, Huang and Haferkamp introduced a con-

struction of pseudoentangled states based on shallow circuits of PFC PRUs—their 1D construction is similar, but not identical, to our MPS construction, and the techniques used in our proofs are different; finally Ref. [46] numerically studied random MPS and PEPS states in the regime of $\chi = \text{poly}(N)$, finding results that become consistent with ours when extrapolated to $\chi = \omega(\text{poly}(N))$.

Acknowledgments. MI gratefully acknowledges discussions with Adam Bouland, Tudor Giurgica-Tiron, and Nick Hunter-Jones.

-
- [1] Ryszard Horodecki and Pawe Horodecki, “Quantum entanglement,” *Rev. Mod. Phys.* **81**, 865–942 (2009).
- [2] Alexei Kitaev and John Preskill, “Topological Entanglement Entropy,” *Physical Review Letters* **96**, 110404 (2006).
- [3] Michael Levin and Xiao-Gang Wen, “Detecting Topological Order in a Ground State Wave Function,” *Physical Review Letters* **96**, 110405 (2006).
- [4] Brian Swingle, “Constructing holographic spacetimes using entanglement renormalization,” [arXiv:1209.3304](https://arxiv.org/abs/1209.3304) (2012), [10.48550/arXiv.1209.3304](https://arxiv.org/abs/10.48550/arXiv.1209.3304).
- [5] J. Maldacena and L. Susskind, “Cool horizons for entangled black holes,” *Fortschritte der Physik* **61**, 781–811 (2013).
- [6] Hong Liu and S. Josephine Suh, “Entanglement Tsunami: Universal Scaling in Holographic Thermalization,” *Physical Review Letters* **112**, 011601 (2014).
- [7] Adam M. Kaufman, M. Eric Tai, Alexander Lukin, Matthew Rispoli, Robert Schittko, Philipp M. Preiss, and Markus Greiner, “Quantum thermalization through entanglement in an isolated many-body system,” *Science* **353**, 794–800 (2016).
- [8] Dmitry A. Abanin, Ehud Altman, Immanuel Bloch, and Maksym Serbyn, “Colloquium: Many-body localization, thermalization, and entanglement,” *Reviews of Modern Physics* **91**, 021001 (2019).
- [9] Scott Aaronson, Adam Bouland, Bill Fefferman, Soumik Ghosh, Umesh Vazirani, Chenyi Zhang, and Zixin Zhou, “Quantum Pseudoentanglement,” [arXiv:2211.00747](https://arxiv.org/abs/2211.00747) (2023), [10.48550/arXiv.2211.00747](https://arxiv.org/abs/10.48550/arXiv.2211.00747).
- [10] Tudor Giurgica-Tiron and Adam Bouland, “Pseudorandomness from Subset States,” [arXiv:2312.09206](https://arxiv.org/abs/2312.09206) (2023), [10.48550/arXiv.2312.09206](https://arxiv.org/abs/10.48550/arXiv.2312.09206).
- [11] Adam Bouland, Bill Fefferman, Soumik Ghosh, Tony Metger, Umesh Vazirani, Chenyi Zhang, and Zixin Zhou, “Public-key pseudoentanglement and the hardness of learning ground state entanglement structure,” [arXiv:2311.12017](https://arxiv.org/abs/2311.12017) (2023), [10.48550/arXiv.2311.12017](https://arxiv.org/abs/10.48550/arXiv.2311.12017).
- [12] Zhengfeng Ji, Yi-Kai Liu, and Fang Song, “Pseudorandom Quantum States,” in *Advances in Cryptology - CRYPTO 2018*, edited by Hovav Shacham and Alexandra Boldyreva (Cham, 2018) pp. 126–152.
- [13] Xiaozhou Feng and Matteo Ippoliti, “Dynamics of Pseudoentanglement,” [arXiv:2403.09619](https://arxiv.org/abs/2403.09619) (2024), [10.48550/arXiv.2403.09619](https://arxiv.org/abs/10.48550/arXiv.2403.09619).
- [14] Adam Bouland, Bill Fefferman, and Umesh Vazirani, “Computational pseudorandomness, the wormhole growth paradox, and constraints on the AdS/CFT duality,” [arXiv:1910.14646](https://arxiv.org/abs/1910.14646) (2019), [10.48550/arXiv.1910.14646](https://arxiv.org/abs/10.48550/arXiv.1910.14646).
- [15] J. Ignacio Cirac, David Perez-Garcia, Norbert Schuch, and Frank Verstraete, “Matrix product states and projected entangled pair states: Concepts, symmetries, theorems,” *Reviews of Modern Physics* **93**, 045003 (2021).
- [16] G. Evenbly and G. Vidal, “Tensor Network States and Geometry,” *Journal of Statistical Physics* **145**, 891–918 (2011).
- [17] Michael P. Zaletel and Frank Pollmann, “Isometric Tensor Network States in Two Dimensions,” *Physical Review Letters* **124**, 037201 (2020).
- [18] Alexander Jahn and Jens Eisert, “Holographic tensor network models and quantum error correction: a topical review,” *Quantum Science and Technology* **6**, 033002 (2021).
- [19] Reza Haghshenas, Johnnie Gray, Andrew C. Potter, and Garnet Kin-Lic Chan, “Variational Power of Quantum Circuit Tensor Networks,” *Physical Review X* **12**, 011047 (2022).
- [20] Tony Metger, Alexander Poremba, Makrand Sinha, and Henry Yuen, “Simple constructions of linear-depth t-designs and pseudorandom unitaries,” [arXiv:2404.12647](https://arxiv.org/abs/2404.12647) (2024).
- [21] Tomohiro Soejima, Karthik Siva, Nick Bultinck, Shubhayu Chatterjee, Frank Pollmann, and Michael P. Zaletel, “Isometric tensor network representation of string-net liquids,” *Physical Review B* **101**, 085117 (2020).
- [22] Maurits S. J. Tepaske and David J. Luitz, “Three-dimensional isometric tensor networks,” *Physical Review Research* **3**, 023236 (2021).
- [23] F. Verstraete, M. M. Wolf, D. Perez-Garcia, and J. I. Cirac, “Criticality, the Area Law, and the Computational Power of Projected Entangled Pair States,” *Physical Review Letters* **96**, 220601 (2006).
- [24] Norbert Schuch, Michael M. Wolf, Frank Verstraete, and J. Ignacio Cirac, “Computational Complexity of Projected Entangled Pair States,” *Physical Review Letters* **98**, 140506 (2007).
- [25] Fernando Pastawski, Beni Yoshida, Daniel Harlow, and John Preskill, “Holographic quantum error-correcting codes: toy models for the bulk/boundary correspondence,” *Journal of High Energy Physics* **2015**, 149 (2015).
- [26] Patrick Hayden, Sepehr Nezami, Xiao-Liang Qi, Nathaniel Thomas, Michael Walter, and Zhao Yang, “Holographic duality from random tensor networks,” *Journal of High Energy Physics* **2016**, 9 (2016).

- [27] Romain Vasseur, Andrew C. Potter, Yi-Zhuang You, and Andreas W. W. Ludwig, “Entanglement transitions from holographic random tensor networks,” *Physical Review B* **100**, 134203 (2019).
- [28] \mathcal{A} is a binary measurement on m copies of the Hilbert space that can be implemented with polynomial resources.
- [29] Don N. Page, “Average entropy of a subsystem,” *Physical Review Letters* **71**, 1291–1294 (1993).
- [30] This approach is also known as “holographic” [47, 48], though not to be confused with the other usage of the word in this paper.
- [31] See Supplementary Information.
- [32] Nicholas Hunter-Jones, “Unitary designs from statistical mechanics in random quantum circuits,” [arXiv:1905.12053](https://arxiv.org/abs/1905.12053) (2019), [10.48550/arXiv.1905.12053](https://arxiv.org/abs/10.48550/arXiv.1905.12053).
- [33] Xiao-Liang Qi, “Exact holographic mapping and emergent space-time geometry,” [arXiv:1309.6282](https://arxiv.org/abs/1309.6282) (2013), [10.48550/arXiv.1309.6282](https://arxiv.org/abs/10.48550/arXiv.1309.6282).
- [34] Xiao-Liang Qi, Zhao Yang, and Yi-Zhuang You, “Holographic coherent states from random tensor networks,” *Journal of High Energy Physics* **2017**, 60 (2017).
- [35] Chris Akers, Netta Engelhardt, Daniel Harlow, Geoff Penington, and Shreya Vardhan, “The black hole interior from non-isometric codes and complexity,” [arXiv:2207.06536](https://arxiv.org/abs/2207.06536) (2022), [10.48550/arXiv.2207.06536](https://arxiv.org/abs/10.48550/arXiv.2207.06536).
- [36] Oliver DeWolfe and Kenneth Higginbotham, “Non-isometric codes for the black hole interior from fundamental and effective dynamics,” [arXiv:2304.12345](https://arxiv.org/abs/2304.12345) (2023), [10.48550/arXiv.2304.12345](https://arxiv.org/abs/10.48550/arXiv.2304.12345).
- [37] Adam Nahum, Jonathan Ruhman, Sagar Vijay, and Jeongwan Haah, “Quantum Entanglement Growth under Random Unitary Dynamics,” *Physical Review X* **7**, 031016 (2017).
- [38] Tianci Zhou and Adam Nahum, “Emergent statistical mechanics of entanglement in random unitary circuits,” *Phys. Rev. B* **99**, 174205 (2019).
- [39] Yaodong Li and Matthew P. A. Fisher, “Statistical mechanics of quantum error correcting codes,” *Physical Review B* **103**, 104306 (2021).
- [40] Yaodong Li, Sagar Vijay, and Matthew P.A. Fisher, “Entanglement Domain Walls in Monitored Quantum Circuits and the Directed Polymer in a Random Environment,” *PRX Quantum* **4**, 010331 (2023).
- [41] Shinsei Ryu and Tadashi Takayanagi, “Holographic Derivation of Entanglement Entropy from the anti-de Sitter Space/Conformal Field Theory Correspondence,” *Physical Review Letters* **96**, 181602 (2006).
- [42] Shinsei Ryu and Tadashi Takayanagi, “Aspects of holographic entanglement entropy,” *Journal of High Energy Physics* **2006**, 045 (2006).
- [43] Chris Akers, Adam Bouland, Lijie Chen, Tamara Kohler, Tony Metger, and Umesh Vazirani, “Holographic pseudoentanglement and the complexity of the AdS/CFT dictionary,” to appear (2024).
- [44] Netta Engelhardt, Asmund Folkestad, Adam Levine, Evita Verheijden, and Lisa Yang, “Spoofing Entanglement in Holography,” [arXiv:2407.14589v1](https://arxiv.org/abs/2407.14589v1) (2024).
- [45] Thomas Schuster, Jonas Haferkamp, and Hsin-Yuan Huang, “Random unitaries in extremely low depth,” [arXiv:2407.07754v1](https://arxiv.org/abs/2407.07754v1) (2024).
- [46] Guglielmo Lami, Jacopo De Nardis, and Xhek Turkeshi, “Anticoncentration and state design of random tensor networks,” [arXiv:2409.13023](https://arxiv.org/abs/2409.13023) (2024), [10.48550/arXiv.2409.13023](https://arxiv.org/abs/10.48550/arXiv.2409.13023).
- [47] Michael Foss-Feig, David Hayes, Joan M. Dreiling, Caroline Figgatt, John P. Gaebler, Steven A. Moses, Juan M. Pino, and Andrew C. Potter, “Holographic quantum algorithms for simulating correlated spin systems,” *Phys. Rev. Research* **3**, 033002 (2021).
- [48] Sajant Anand, Johannes Hauschild, Yuxuan Zhang, Andrew C. Potter, and Michael P. Zaletel, “Holographic Quantum Simulation of Entanglement Renormalization Circuits,” *PRX Quantum* **4**, 030334 (2023).
- [49] Benoit Collins and Sho Matsumoto, “Weingarten calculus via orthogonality relations: new applications,” *Latin American Journal of Probability and Mathematical Statistics* **14**, 631 (2017).

Supplementary Information: Pseudoentanglement from tensor networks

Zihan Cheng, Xiaozhou Feng, and Matteo Ippoliti
Department of Physics, The University of Texas at Austin, Austin, TX 78712, USA

CONTENTS

S1. Bounds on Weingarten functions	1
S2. Computational indistinguishability between $\mathcal{E}_{\text{pMPS}'}$ and $\mathcal{E}_{\text{rMPS}}$	2
S3. Proof of pseudorandomness for arbitrary isometric tensor network geometries	3
A. Setup	3
B. Generalization of Lemma 1	3
C. Generalization of Lemma 2	4
1. Uniform spin configurations	4
2. Non-uniform spin configurations	4
S4. Proof of Ryu-Takayanagi formula for pseudoentangled holographic tensor network	5

S1. BOUNDS ON WEINGARTEN FUNCTIONS

Here we prove several facts about the Weingarten function which are used in the main text toward proving Theorem 1. To this end, it is helpful to first recall the relationship between Weingarten functions and the Gram matrix of permutations, $G_{\sigma,\tau} \equiv \text{Tr}(\hat{\sigma}\hat{\tau}^{-1}) = d^{|\sigma\tau^{-1}|}$. Here d is the dimension of the underlying Hilbert space, $\sigma, \tau \in S_m$ are permutations, m is the number of copies (or replicas) of the Hilbert space, and $|\sigma| \in \{1, \dots, m\}$ denotes the number of cycles in permutation σ . We have $\text{Wg}_d(\sigma\tau^{-1}) = (G^{-1})_{\sigma,\tau}$, with G^{-1} the matrix inverse of G , viewed as a $m! \times m!$ square matrix. The matrix is invertible as long as $m < d$, which is the regime of interest to us.

Fact S1.1. *We have $\sum_{\beta \in S_m} d^{|\beta|} = d^m [1 + O(m^2/d)]$.*

Proof. Noting that $d^{|\beta|} = \text{Tr}(\hat{\beta})$, where $\hat{\beta}$ is the replica permutation operator associated to $\beta \in S_m$, we have

$$\sum_{\beta \in S_m} d^{|\beta|} = \text{Tr} \left(\sum_{\beta \in S_m} \hat{\beta} \right) = m! \text{Tr}(\hat{\Pi}_{\text{sym}}) = \frac{(d-1+m)!}{(d-1)!}, \quad (\text{S1})$$

where $\hat{\Pi}_{\text{sym}} = (1/m!) \sum_{\beta} \hat{\beta}$ is the projector on the symmetric sector of the m -copy Hilbert space, which has dimension $\binom{d-1+m}{m}$. The statement follows from the ‘birthday statistics’: $\log[(d-1+m)!/(d-1)!] = m \log(d-1) + \binom{m}{2} \frac{1}{d-1} + o(1/d)$. \square

Fact S1.2. *We have $\sum_{\beta \in S_m} d^m \text{Wg}_d(\beta) = 1 + O(m^2/d)$.*

Proof. We have that $1 = \text{Tr} \mathbb{E}_{U \sim \text{Haar}} [U^{\otimes m} |0\rangle\langle 0| (U^\dagger)^{\otimes m}] = \sum_{\sigma, \tau \in S_m} \text{Wg}_d(\tau\sigma^{-1}) d^{|\sigma|}$. Changing summation variable to $\tau \mapsto \tau' = \tau\sigma^{-1}$ yields

$$\sum_{\tau' \in S_m} \text{Wg}_d(\tau') = \left(\sum_{\sigma \in S_m} d^{|\sigma|} \right)^{-1} = \frac{(d-1)!}{(d-1+m)!} = d^{-m} [1 + O(m^2/d)] \quad (\text{S2})$$

by Fact S1.1. \square

Fact S1.3. *For all permutations $\sigma \in S_m$, we have*

$$|\text{Wg}_d(\sigma)| = d^{|\sigma|-2m} f(\sigma) [1 + O(m^2/d)], \quad (\text{S3})$$

with $f(\sigma) = \prod_{i=1}^{|\sigma|} \frac{1}{\ell_i} \binom{2(\ell_i-1)}{\ell_i-1}$, and $\{\ell_i\}_{i=1}^{|\sigma|}$ the lengths of all cycles in σ . In particular $\text{Wg}_d(e) = d^{-m} [1 + O(m^2/d)]$.

Proof. See Ref. [49]. Note that our usage of the notation for $|\sigma|$ differs from theirs. The second statement follows from the fact that e has m cycles of length 1, so $f(e) = 1$. \square

Fact S1.4. We have $\sum_{\beta \in S_m} d^m |\mathbf{Wg}_d(\beta)| = 1 + O(m^2/d)$.

Proof. First we have a lower bound $\sum_{\beta \in S_m} d^m |\mathbf{Wg}_d(\beta)| \geq \sum_{\beta \in S_m} d^m \mathbf{Wg}_d(\beta) = 1 + O(m^2/d)$, by Fact S1.2. Second, we can prove an upper bound by invoking Fact S1.3:

$$\begin{aligned} \sum_{\beta \in S_m} d^m |\mathbf{Wg}_d(\beta)| &\leq [1 + O(m^2/d)] \sum_{\beta \in S_m} d^{|\beta| - m} f(\beta) \\ &\leq [1 + O(m^2/d)] \sum_{\beta \in S_m} (d/4)^{|\beta| - m} \\ &\leq 1 + O(m^2/d). \end{aligned} \tag{S4}$$

In the second inequality we used the fact that $\frac{1}{\ell} \binom{2(\ell-1)}{\ell-1} \leq 4^{\ell-1}$, so that $f(\beta) \leq 4^{\sum_i (\ell_i - 1)} = 4^{m - |\beta|}$. We then used Fact S1.1 to carry out the sum over β . \square

S2. COMPUTATIONAL INDISTINGUISHABILITY BETWEEN $\mathcal{E}_{\text{pMPS}'}$ AND $\mathcal{E}_{\text{rMPS}}$

Here we give a proof of Lemma 1, stating the indistinguishability between the ensemble of MPS made out of Haar-random gates, $\mathcal{E}_{\text{rMPS}}$, and the analogous ensemble where the MPS is made out of random ‘PFC’ gates, $\mathcal{E}_{\text{pMPS}'}$. To this end, we use a key property of the PFC ensemble:

Fact S2.1. Given an arbitrary state ρ on $\mathcal{H}_A^{\otimes m} \otimes \mathcal{H}_B$, with \mathcal{H}_A a Hilbert space of dimension d and \mathcal{H}_B an arbitrary Hilbert space, we have

$$\|\Phi_{\text{Haar}}^{(m)} \otimes \mathcal{I}(\rho) - \Phi_{\text{PFC}}^{(m)} \otimes \mathcal{I}(\rho)\|_{\text{tr}} \leq O(m/\sqrt{d}), \tag{S5}$$

where $\Phi_{\text{Haar}}^{(m)} \otimes \mathcal{I}(\rho) = \mathbb{E}_{U \sim \text{Haar}}[(U^{\otimes m} \otimes I)\rho(U^{\otimes m} \otimes I)^\dagger]$ is the m -fold twirling channel for the Haar ensemble (acting only on the $\mathcal{H}_A^{\otimes m}$ factor of the Hilbert space), and $\Phi_{\text{PFC}}^{(m)}$ is the same for the PFC ensemble.

Proof. See Ref. [20], Theorem 5.2. Note that the theorem is proven for pure states; we can obtain this statement by expanding the auxiliary Hilbert space \mathcal{H}_B to purify ρ , and using monotonicity of the trace distance under the partial trace. \square

The moment operators for the two ensembles $\mathcal{E}_{\text{pMPS}'}$, $\mathcal{E}_{\text{rMPS}}$ can be written as

$$\rho_{\mathcal{E}_{\text{rMPS}}}^{(m)} = \Phi_{\text{Haar}}^{(m)}|_{[L, L+\nu]} \circ \Phi_{\text{Haar}}^{(m)}|_{[L-1, L+\nu-1]} \circ \cdots \circ \Phi_{\text{Haar}}^{(m)}|_{[1, \nu+1]}(\rho_0), \tag{S6}$$

$$\rho_{\mathcal{E}_{\text{pMPS}'}}^{(m)} = \Phi_{\text{PFC}}^{(m)}|_{[L, L+\nu]} \circ \Phi_{\text{PFC}}^{(m)}|_{[L-1, L-1+\nu]} \circ \cdots \circ \Phi_{\text{PFC}}^{(m)}|_{[1, \nu+1]}(\rho_0), \tag{S7}$$

where $\rho_0 = (|0\rangle\langle 0|)^{\otimes mN}$ is the m -fold replicated input state and $\Phi^{(m)}|_{[i, j]}$ denotes an m -fold twirling channel acting only on qubits i through j on the chain (the identity channel on all other qubits is implicit). In our staircase circuits, gates act on $\nu + 1$ consecutive qubits and move over by 1 qubit at each time step.

We aim to prove that

$$\|\rho_{\mathcal{E}_{\text{rMPS}}}^{(m)} - \rho_{\mathcal{E}_{\text{pMPS}'}}^{(m)}\|_{\text{tr}} \leq L\epsilon, \tag{S8}$$

with ϵ the approximation error of the PFC ensemble on $\nu + 1$ qubits: $\epsilon \leq O(m/\sqrt{\chi})$, where $\chi = 2^\nu$ is the MPS bond dimension. We will prove the statement by induction.

- ($L = 1$): The whole system consists of $\nu + 1$ qubits. We have $\|\Phi_{\text{Haar}}^{(m)}(\rho_0) - \Phi_{\text{PFC}}^{(m)}(\rho_0)\|_{\text{tr}} \leq \epsilon$.
- ($L - 1 \implies L$): Let

$$\rho_1 = \Phi_{\text{Haar}}^{(m)}|_{[L-1, L-1+\nu]} \circ \cdots \circ \Phi_{\text{Haar}}^{(m)}|_{[1, \nu+1]}(\rho_0), \tag{S9}$$

$$\rho_2 = \Phi_{\text{PFC}}^{(m)}|_{[L-1, L-1+\nu]} \circ \cdots \circ \Phi_{\text{PFC}}^{(m)}|_{[1, \nu+1]}(\rho_0). \tag{S10}$$

We have, by triangle inequality,

$$\begin{aligned} \|\Phi_{\text{Haar}}^{(m)}|_{[L,L+\nu]}(\rho_1) - \Phi_{\text{PFC}}^{(m)}|_{[L,L+\nu]}(\rho_2)\|_{\text{tr}} &\leq \|\Phi_{\text{Haar}}^{(m)}|_{[L,L+\nu]}(\rho_1) - \Phi_{\text{PFC}}^{(m)}|_{[L,L+\nu]}(\rho_1)\|_{\text{tr}} \\ &+ \|\Phi_{\text{PFC}}^{(m)}|_{[L,L+\nu]}(\rho_1) - \Phi_{\text{PFC}}^{(m)}|_{[L,L+\nu]}(\rho_2)\|_{\text{tr}}. \end{aligned} \quad (\text{S11})$$

The first term on the rhs is $\leq \epsilon$ by direct application of Eq. (S5). The second term, by monotonicity of the trace distance under quantum channels, is $\|\Phi_{\text{PFC}}^{(m)}(\rho_1 - \rho_2)\|_{\text{tr}} \leq \|\rho_1 - \rho_2\|_{\text{tr}}$; but (up to tensoring with a trivial state $|0\rangle\langle 0|^{\otimes m}$) $\rho_1 - \rho_2$ is the difference between the two moment operators at step $L - 1$, which by hypothesis is $\leq (L - 1)\epsilon$. The result follows.

We remark that this proof did not use the MPS structure specifically, but only the isometric structure of the tensor network (i.e. the ability to write it as a sequential application of unitary gates). As long as the network consists of $\text{poly}(N)$ gates, the error incurred by replacing Haar-random gates by PFC gates remains small, $O(\text{poly}(N)m/\sqrt{\chi})$.

S3. PROOF OF PSEUDORANDOMNESS FOR ARBITRARY ISOMETRIC TENSOR NETWORK GEOMETRIES

Here we modify the proof presented in the main text for MPS to general isometric tensor network architectures.

A. Setup

Formally, we consider a weighted directed graph whose edges are qudit worldlines (with the direction of each edge going from past to future and the weight indicating the bond dimension χ_i , allowed to vary across edges) and whose vertices can be of three types: unitary, input, or output.

- (i) Unitary vertices must have both incoming and outgoing edges, and must respect the condition $\prod_{i \in \text{incoming}} \chi_i = \prod_{i \in \text{outgoing}} \chi_i$ (unitarity).
- (ii) Input vertices have only outgoing legs. We restrict for simplicity to product states $|0\rangle$, which have one outgoing edge, and Bell pairs $|\psi_{\text{Bell}}\rangle = (1/\sqrt{\chi}) \sum_{j=0}^{\chi-1} |jj\rangle$, which have two outgoing edges of the same bond dimension χ . Both types of input vertices are illustrated in Fig. 2(a,c).
- (iii) Output vertices have only one incoming edge and no outgoing edges. They represent ‘‘dangling legs’’ in standard tensor network notation.

N is the number of output vertices. We assume that the total number of unitary vertices in the graph is $n_U \leq O(\text{poly}(N))$. This ensures the states’ efficient preparability.

We aim to prove that the states obtained from these graphs by placing a PFC gate of the appropriate dimension on each unitary vertex are computationally indistinguishable from Haar-random states of dimension $D = \prod_{\ell \in \text{output}} \chi_\ell$, where the product runs over edges connected to output vertices. (Each output vertex represents a local Hilbert space and the output state lives in the tensor product of these spaces.)

The proof is analogous to the one reported in the main text for matrix product states, with some small modifications that we address in the following.

B. Generalization of Lemma 1

We can repeat the same argument as in Sec. S2, but instead of $O(N\epsilon)$ as the upper bound we obtain $O(\sum_{u \in \text{gates}} \epsilon_u)$, since in this case each gate may act on a Hilbert space of different dimension. We have $\epsilon_u \leq O(m^2/d_u)$, with $d_u = \prod_{\ell \in \text{outgoing}(u)} \chi_\ell$, and thus

$$\|\rho_{\mathcal{E}_{\text{PTNS}}}^{(m)} - \rho_{\mathcal{E}_{\text{rTNS}}}^{(m)}\|_{\text{tr}} \leq O(n_U m / \sqrt{d_{\min}}), \quad d_{\min} = \min_u \prod_{\ell \in \text{outgoing}(u)} \chi_\ell. \quad (\text{S12})$$

Here n_U is the total number of unitary gates in the network, again assumed to be $O(\text{poly}(N))$.

C. Generalization of Lemma 2

We can now perform the Haar averages and obtain a modified graph corresponding to the partition functions in Fig. 2(b,d). The new graph is undirected, weighted and labeled—each edge has one of two labels, that we denote by ‘solid’ and ‘dashed’ in keeping with Fig. 1 and Fig. 2. The new graph is built according to these rules:

- All edges between two unitary vertices become ‘solid’ and keep their weight.
- Output vertices and their incoming edges are removed.
- Input vertices are removed. For input vertices of product-state type, the outgoing edge is also removed. For input vertices of Bell-pair type, the outgoing edges are merged into a single ‘solid’ edge whose weight is still χ .
- Each unitary vertex is replaced by two vertices. One is connected to all the formerly outgoing edges, the other to all the formerly incoming edges. The two vertices are connected to each other by a new ‘dashed’ edge of weight d_u (Hilbert space dimension on which the unitary acts).

This graph serves as the interaction graph for the S_m -valued magnet’s partition function: each vertex hosts a spin $\alpha \in S_m$, each edge connecting two spins $\alpha_{i,j}$ contributes a Boltzmann weight $\chi_\ell^{|\alpha_i \alpha_j^{-1}|}$ if it is ‘solid’, $\text{Wg}_{d_u}(\alpha_i \alpha_j^{-1})$ if it is ‘dashed’, with χ_ℓ and d_u the edge weights as defined above. In addition, there is an overall prefactor of $\prod_{\ell \in \text{Bell}} \chi_\ell^{-m}$, with the product running over Bell pair input states in the original graph, coming from the normalization prefactor in $|\psi_{\text{Bell}}\rangle\langle\psi_{\text{Bell}}|^{\otimes m}$.

The proof of computational indistinguishability proceeds in the same way as for the MPS case until the derivation of Eqs. (3-4).

1. Uniform spin configurations

To prove that Δ_m^u is small, Eq. (5), we need to show that the Boltzmann weight $e^{-E[\{e,e\}]}$ of a uniform spin configuration is close to D^{-m} . We have

$$\begin{aligned} e^{-E[\{e,e\}]} &= \prod_{\ell \in \text{Bell}} \chi_\ell^{-m} \prod_{\ell \in \text{solid}} \chi_\ell^m \prod_{u \in \text{dashed}} \text{Wg}_{d_u}(e) \\ &= \prod_{\substack{\ell \in \text{solid,} \\ \text{not Bell}}} \chi_\ell^m \prod_{u \in \text{dashed}} d_u^{-m} [1 + O(m^2/d_u)], \end{aligned} \quad (\text{S13})$$

where we used the results of Sec. S1 to approximate the Weingarten functions, and restricted the product over edges to edges that did not originate from Bell pairs. Now, viewing d_u as the product of χ_ℓ over outgoing legs of the unitary, we have that each leg connecting two unitaries gives both a factor of χ^{+m} (from the first term in Eq. (S13)) and a factor of χ^{-m} (from the second term), which cancel. The only factors to not cancel are χ^{-m} for legs in the original graph that do *not* terminate at a unitary. These legs can only terminate at output vertices, so in all the result is $(\prod_{\ell \in \text{output}} \chi_\ell)^{-m} = D^{-m}$, with D the physical Hilbert space dimension. The error terms stem only from the Weingarten functions and can be bounded above by $|[1 + O(m^2/d_u)]^{n_U} - 1|$ with n_U the number of unitaries. Overall this gives

$$\Delta_m^u \leq O(n_U m^2 / d_{\min}), \quad (\text{S14})$$

which is smaller than the error incurred from the replacing pseudorandom with Haar-random gates, Eq. (S12).

2. Non-uniform spin configurations

The derivation of (7) makes no reference to the MPS structure and thus proceeds unchanged. Once we have a partition function with positive Boltzmann weights

$$e^{-(E^+[\{\sigma'_i, \tau_i\}] - E^+[\{e,e\}])} = \prod_{(i,j) \in \text{edges}} \begin{cases} 1 & \text{if } \alpha_i = \alpha_j, \\ O(1/\chi_{ij}) & \text{otherwise.} \end{cases} \quad (\text{S15})$$

we can bound it above by simply dropping edges—i.e. setting the associated factor to 1 regardless of the spins $\alpha_{i,j}$. Dropping edges until we obtain a spanning tree \mathcal{T} of the graph, as sketched in Fig. 2(b,d), and moving to bond variables $\beta_{ij} \equiv \alpha_i \alpha_j^{-1}$ starting from the pinned site $\sigma'_1 = e$ and covering all links in the spanning tree, we get

$$\begin{aligned} \sum_{\{\sigma'_i, \tau_i\} \text{ n.u.}} e^{-(E^+[\{\sigma'_i, \tau_i\}] - E^+[\{e, e\}])} &\leq \prod_{\ell \in \mathcal{T}, \text{ solid}} \left(\sum_{\beta} \chi_{\ell}^{|\beta| - m} \right) \prod_{\ell \in \mathcal{T}, \text{ dashed}} \left(\sum_{\beta} \frac{|\text{Wg}_{d_{\ell}}(\beta)|}{\text{Wg}_{d_{\ell}}(e)} \right) - 1 \\ &\leq \prod_{\ell \in \mathcal{T}, \text{ solid}} [1 + O(m^2/\chi_{\ell})] \prod_{\ell \in \mathcal{T}, \text{ dashed}} [1 + O(m^2/d_{\ell})] - 1 \\ &\leq O(n_E m^2/\chi_{\min}) + O(n_U m^2/d_{\min}). \end{aligned} \quad (\text{S16})$$

Here χ_{\min} is the minimum bond dimension of an inner bond (i.e., a bond connecting unitary gates—physical bonds are excluded), and n_E is the number of inner bonds. We have that $d_{\min} \geq \chi_{\min}$ and that $n_E = \Theta(n_U)$, so we can simplify the error term as $\leq O(n_U m^2/\chi_{\min})$. This may be larger or smaller than the error incurred from replacing pseudorandom gates with Haar-random gates, Eq. (S12), depending on the connectivity of the circuit, i.e. whether $\chi_{\min} < \sqrt{d_{\min}}$ or not.

In summary, we conclude that

$$\|\rho_{\mathcal{E}_{\text{PTNS}}}^{(m)} - \rho_{\mathcal{E}_{\text{Haar}}}^{(m)}\|_{\text{tr}} \leq O(n_U m^2/\chi_{\min}) + O(n_U m/\sqrt{d_{\min}}). \quad (\text{S17})$$

For the case of uniform inner bond dimension χ across the network and $n_U = O(N)$, this yields the MPS result: $O(Nm^2/\sqrt{\chi})$. However this shows that the result is much more general, and that arbitrary isometric tensor network geometries still yield computationally random states as long as n_U is not too large and there are no “weak links” where χ or d_u become too small.

S4. PROOF OF RYU-TAKAYANAGI FORMULA FOR PSEUDOENTANGLED HOLOGRAPHIC TENSOR NETWORK

Here we prove a lower bound on the average entropy $S(A)$ of a subsystem A in the pseudorandom holographic tensor network ensemble, $\mathcal{E}_{\text{holo}}$, considered in the main text. Our strategy for lower-bounding $S(A)$ is to evaluate the average purity, $\mathbb{E}[\text{Tr}(\rho_A^2)]$. Indeed we have the following:

Fact S4.1. *We have, in general, $-\log \mathbb{E}[\text{Tr}(\rho_A^2)] \leq \mathbb{E}[S(A)]$.*

Proof. First, by convexity, we have $\mathbb{E}[-\log(x)] \geq -\log \mathbb{E}[x]$, and thus

$$-\log \mathbb{E}[\text{Tr}(\rho_A^2)] \leq \mathbb{E}[-\log \text{Tr}(\rho_A^2)] = \mathbb{E}[S_2(A)], \quad (\text{S18})$$

where we identified the second Renyi entropy $S_2(A) = -\log \text{Tr}(\rho_A^2)$. Secondly, the well known monotonicity of the Renyi entropies $S_n(A)$ vs the index n , and the fact that $S(A) = \lim_{n \rightarrow 1} S_n(A)$, gives $S_2(A) \leq S(A)$ in general, and thus $\mathbb{E}[S(A)] \geq \mathbb{E}[S_2(A)]$. \square

In the following we treat the unitary gates as if they are genuinely Haar-random: since the average purity is a second-moment quantity, this is justified by noting that the PFC ensemble forms an exact two-design (due to the random Clifford operation that is part of the PFC sequence). The average purity for our tensor network states is given by a partition function of spins valued in $S_2 = \{e, s\}$:

$$\text{Tr}(\rho_A^2) = \sum_{\{\sigma_i, \tau_i \in S_2\}} e^{-E_{A, \bar{A}}[\{\sigma_i, \tau_i\}]}, \quad (\text{S19})$$

where the energy term $E_{A, \bar{A}}[\{\sigma_i, \tau_i\}]$ comprises both bulk terms (overlaps or Weingarten functions between neighboring permutations) and boundary terms (overlaps between σ 's and e in A , and between σ 's and s in \bar{A} , respectively). Since we are interested in an upper bound on the purity (i.e. a lower bound on the entropy), we can switch to positive Boltzmann weights:

$$\text{Tr}(\rho_A^2) \leq \sum_{\{\sigma_i, \tau_i \in S_2\}} \left| e^{-E_{A, \bar{A}}[\{\sigma_i, \tau_i\}]} \right| = \sum_{\{\sigma_i, \tau_i \in S_2\}} e^{-E_{A, \bar{A}}^+[\{\sigma_i, \tau_i\}]}, \quad (\text{S20})$$

The graph contains two types of bonds: overlaps between permutations (solid lines in Fig. 2(d)) and Weingarten functions (dashed lines in Fig. 2(d)). There are n_o of the former type and n_w of the latter. The overlaps contribute a factor of either χ^2 (if the two permutations they connect are the same) or χ (if they are opposite); the Weingarten functions are either $(\chi^6 - 1)^{-1}$ or $\chi^{-1}(\chi^6 - 1)^{-1}$ respectively. We factor out a χ^2 from each of the n_o overlap bonds and $(\chi^6 - 1)^{-1}$ from each of the n_w Weingarten bonds. In all, this gives a factor of $\chi^{2n_o}/(\chi^6 - 1)^{n_w}$; since $n_w = 3n_o$ (from a counting of total number of legs in the network), we get

$$\text{Tr}(\rho_A^2) \leq (1 - \chi^{-6})^{n_w} \sum_{\{\sigma_i, \tau_i \in S_2\}} e^{-\delta E_{A, \bar{A}}^+[\{\sigma_i, \tau_i\}]} \leq [1 + O(N/\chi^6)] \sum_{\{\sigma_i, \tau_i \in S_2\}} e^{-\delta E_{A, \bar{A}}^+[\{\sigma_i, \tau_i\}]}.$$
 (S21)

The energy terms are now normalized in such a way that they contribute a factor of 1 if the two permutations are equal, and $1/\chi$ or $1/\chi^3$ respectively if the permutations are different. Since the partition function depends only on the relative value of neighboring spins, if we include (pinned) spins at the boundary (s in A and e in \bar{A}) then the sum over site variables $\{\sigma_i, \tau_i\}$ can be rewritten in terms cuts γ through the bonds of the network, with

$$\text{Tr}(\rho_A^2) \leq [1 + O(N/\chi^6)] \sum_{\text{cuts } \gamma} \chi^{-|\gamma|},$$
 (S22)

and $|\gamma|$ the number of bonds cut by γ (with the convention that cutting a Weingarten link contributes 3 bonds in this case). This is already a RT formula with a fluctuating cut. Then, owing to the large bond dimension χ , fluctuations of the cut are suppressed and one obtains ‘minimum-cut’ prescription. To this end, let us (very loosely) upper bound the number of possible cuts of a given length ℓ as $\binom{n_b}{\ell}$, with $n_b = n_e + n_o$ the total number of bonds in the network (on hyperbolic tilings, where bulk and boundary scale in the same way, we have $n_b = O(N)$). Then, letting $\ell_{\min} = \min_{\gamma_A} |\gamma_A|$, we have

$$\text{Tr}(\rho_A^2) \leq [1 + O(N/\chi^6)] \sum_{\ell=\ell_{\min}}^{n_b} \binom{n_b}{\ell} \chi^{-\ell} \leq [1 + O(N/\chi^6)] \sum_{\ell=\ell_{\min}}^{\infty} (n_b/\chi)^\ell$$
 (S23)

$$\leq \frac{1 + O(N/\chi^6)}{1 - (n_b/\chi)} (n_b/\chi)^{\ell_{\min}}$$
 (S24)

Finally, we arrive at the desired bound:

$$\mathbb{E}[S(A)] \geq -\log \mathbb{E}[\text{Tr}(\rho_A^2)] \geq \ell_{\min} \log \frac{\chi}{n_b} + \log(1 + O(N/\chi))$$
 (S25)

$$\geq \ell_{\min} \log(\chi) \left[1 - \frac{\log n_b}{\log \chi} \right] + O(N/\chi)$$
 (S26)

Since $n_b = O(N)$ and $\log \chi = \omega(\log N)$, we have $\log(n_b)/\log(\chi) = o(1)$ (vanishing in the thermodynamic limit). This gives the result quoted in the main text.

Nothing in this proof specifically hinges on the choice of holographic network; e.g., all the steps would work analogously for arbitrary tilings of the hyperbolic plane that admit an isometric realization (e.g. this includes all tensors with an even number of legs, and potentially other cases with suitable choices of bond dimensions).